Small and medium-scale focused research project "SUCCESS"

Deliverable

D5.1

Final Report on AiP Solutions

Contractual data:	**M36**
Actual data:	**M40**
Authors:	**Stefan Beer (KIT)**
Participants:	**KIT, SELMIC, Hightec, Bosch**
Work package:	**WP5**
Security:	**Public**
Nature:	**Report**
Version:	**1.0**
Total number of pages:	**21**

Abstract

EU-STREP Project SUCCESS

Deliverable D5.1 (WP5). This document reports on the final antenna in package solutions for the fully integrated 122 GHz radar sensors. Measurement and simulation results of antennas including the chip interconnects are given. System in Package prototypes are shortly explained with a focus on the antennas.

Keywords

Integrated antennas, plastic packaging, millimeter wave, integrated system, 122GHz

SUCCESS Consortium

This document is part of a research project funded by the Framework Program 7 of the Commission of the European Union.

IHP GMBH IHP Im Technologiepark 25 15236 Frankfurt (Oder) Germany	ROBERT BOSCH GMBH RB Robert-Bosch-Platz 1 70839 Gerlingen-Schillerhöhe Germany
STMICROELECTRONICS S.A. ST Boulevard Romain Rolland 29 92120 Montrouge France	KARLSRUHE INSTITUTE OF TECHNOLOGY KIT Kaiserstrasse 12 76131 Karlsruhe Germany
SILICON RADAR GMBH SR Im Technologiepark 25 15236 Frankfurt (Oder) Germany	SELMIC OY SELMIC Veistamotie 15 FI-90550 Oulu Finland
HIGHTEC MC AG HIT Fabrikstrasse 9 5600 Lenzburg Switzerland	EVATRONIX IP EVA Przybyly 2 43-300 Bielsko-Biala Poland
UNIVERSITY OF TORONTO UoT Kings College Circle 27 M5S 1A1 Toronto Canada	

Table of Contents

1. AiP Solution using Wire Bonding

1.1. Packaging concept

A wire bonded solution for a System-in-Package is depicted in Figure 1. Inside the standard QFN package, consisting out of a package base and a molded cap, the MMIC is just placed next to the antenna substrate. The interconnections are all realized by bond wires, which connect the leads with the MMIC (low frequency connection) and the MMIC with the antenna feeding line (RF connection). This concept is the easiest in terms of assembly effort. The main effort has to be put in accurately controlling the length of the 122 GHz wire-bond interconnect between the MMIC and the antenna. This also means that the MMIC and the antenna have to be positioned auite accurately.

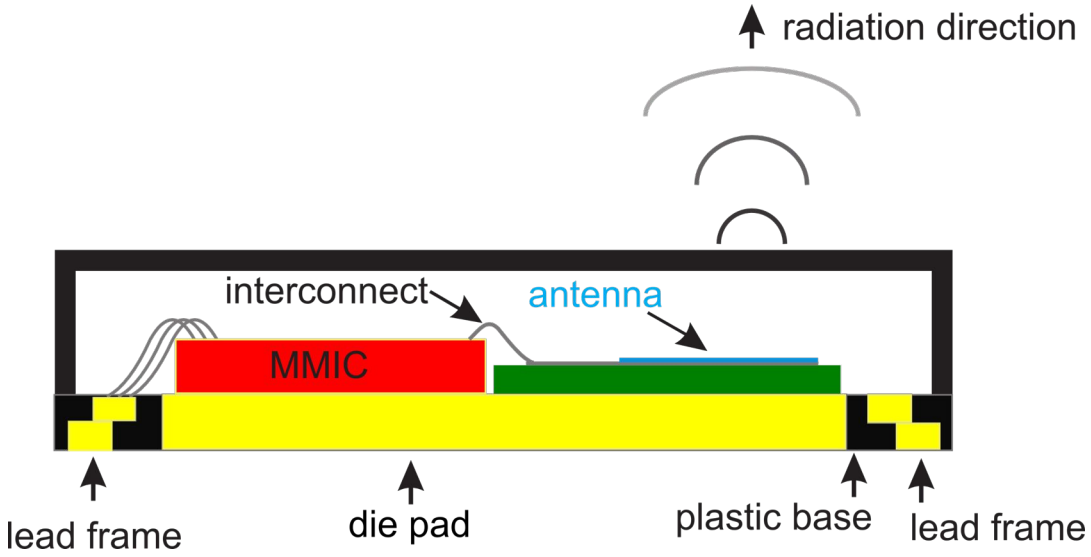

Figure 1: Concept with wire-bond interconnect and printed antenna besides MMIC

1.2. Antenna Array with a grounded Coplanar Waveguide Feed

1.2.1. Material selection

An integrated antenna array that uses an air cavity below the substrate to enhance its bandwidth was shown in a previous work [1], [3]. Though this antenna shows an excellent behaviour, it leads to a more complicated assembly process. The air cavity has to be milled or etched, and later it must be kept free of adhesives. If a reduced impedance bandwidth is acceptable, an antenna without an air cavity can be used. This leads to a simplified assembly process as it can simply be die bonded into the package. Another benefit of not using an air cavity below the antenna substrate is that a flexible material is usable.

Rogers Ultralam 3850 is used as antenna substrate as it has a low permittivity and low losses up to the millimeter-wave range [4], [5]. The available maximum thickness of 0.1 mm is used to achieve the highest bandwidth for the antenna. The principle antenna design that is shown in the following can also be transferred to other low permittivity substrates.

As both the antenna design at 122 GHz and the bond wire compensation [2] requires tight line and space widths in the range of 20µm, the substrate had to be processed in thin film technology. Therefore the 19 µm thick copper layer on the top of the substrate was completely removed using an etching process. Afterwards, a thin film process was used to structure the metallization on the top of the substrate. A 3 µm copper layer is used on an undercoating. On top of the copper, a 0.5 µm gold layer is used to facilitate wire bonding.

1.2.2. Antenna Array Design

A top view of the antenna array is shown in Figure 2. The array is composed of four elements that are fed by a novel feeding network using a grounded Coplanar Wave-

guide (GCPW), and pairs of coupled microstrip (MS) lines.

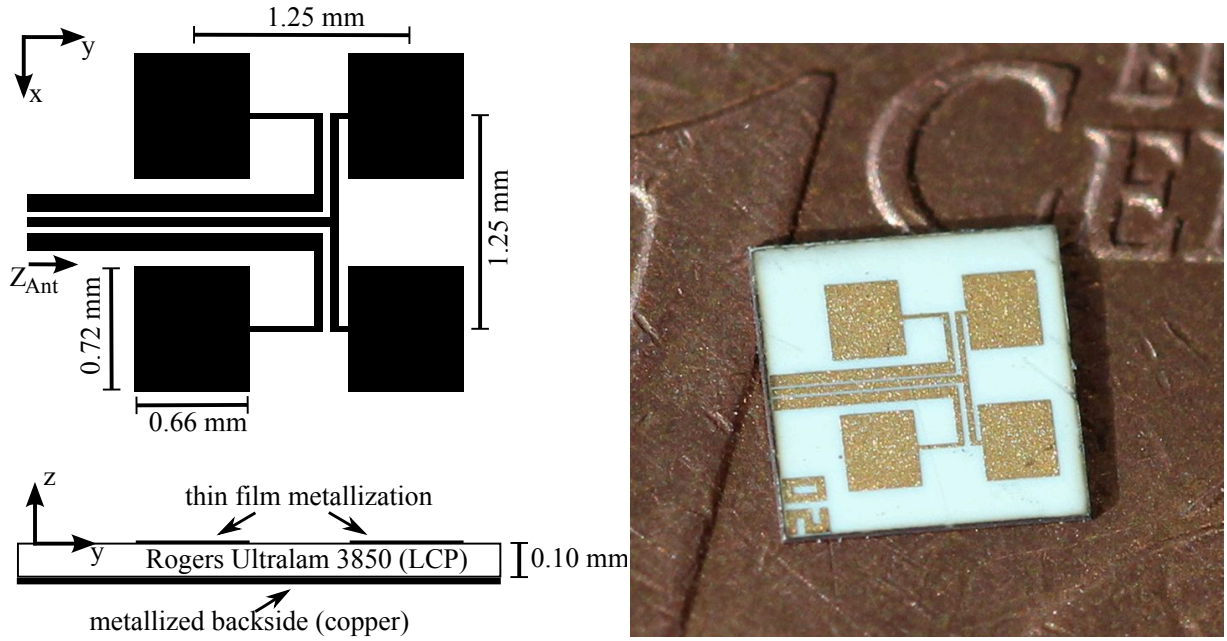

Figure 2 Antenna array with GCPW-feeding on 0.1 mm thick Rogers Ultralam 3850

Usually, planar patch arrays are either fed using parallel or serial MS feeding networks [6]. A disadvantage of a parallel feeding is that a certain space is needed for the feeding lines between the radiating elements. Thus the single elements often have to be positioned with spacings larger than half a freespace wavelength. Another drawback of conventional MS feeding networks is the necessity of a transition between the GCPW-line that is formed by the three bond pads and the MS line. The feeding network that is used in the present work has several advantages: No transition is needed; the bond wire matching circuits [2] can perfectly be integrated into the feeding line; and the available space is used optimally for the radiating elements as the complete feeding network is realized in between the antenna elements.

1.2.3. Simulation and Measurement Results of the Antenna

The antenna was measured with a probe based antenna measurement setup at KIT [7]. The setup allows calibrated measurements of the antenna impedance, as well as its radiation patterns and gain. Figure 3 shows a comparison of the measured and simulated reflection coefficient. A very good agreement can be observed. In measurements, a –10 dB-bandwidth of 119.1 GHz to 125.7 GHz and thus 5.4% is achieved.

This is considerably higher compared to the required bandwidth of 122 GHz to 123 GHz. By using a thicker substrate an even higher bandwidth could be achieved.

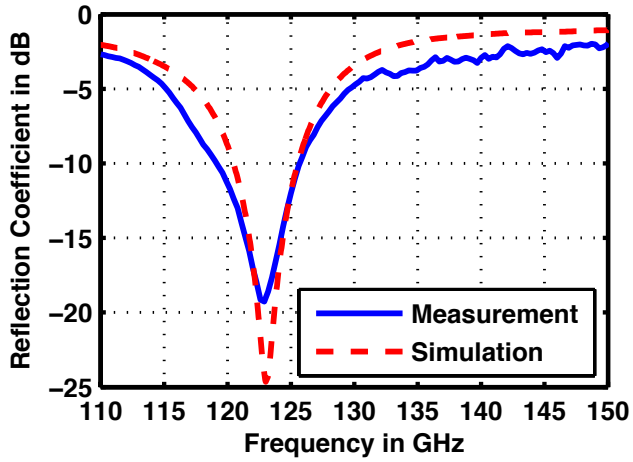

Figure 3 Simulated and measured reflection coefficient of the antenna

The measured and simulated radiation patterns are shown in Figure 4. Apart from a slight unbalance, the H-plane pattern shows an excellent agreement. The measurements in the E- plane show some sidelobes in the angular range around 60° that can be attributed to reflections at the metallic waveguide probe. This waveguide probe also leads to a shadowing in the E-plane pattern below −15°. The measured and simulated gain is 11.0 dBi and 11.3 dBi, respectively. Thus it can be concluded that the simulated antenna efficiency of 85% is a realistic value.

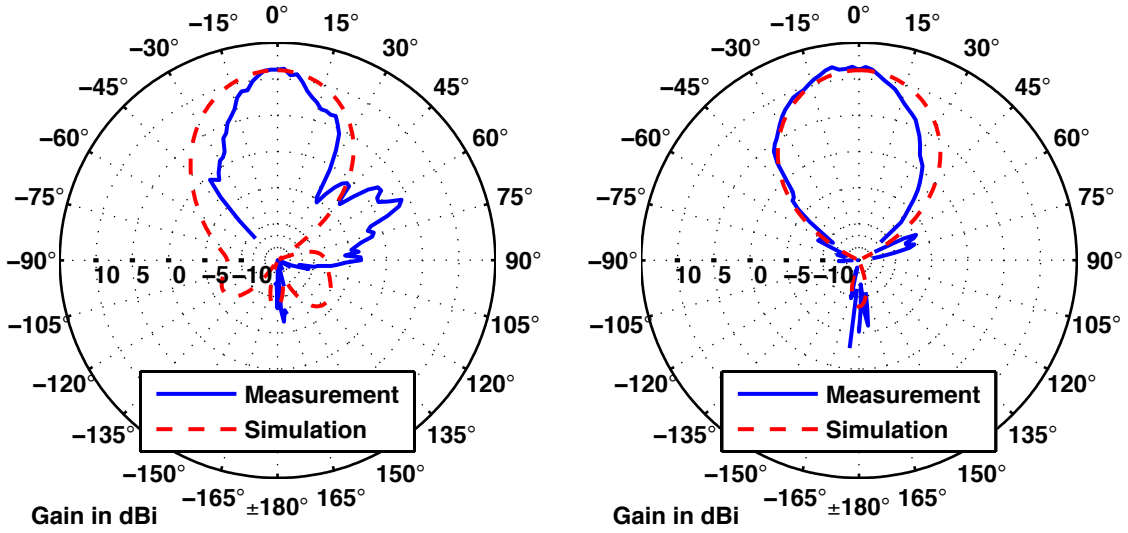

Figure 4 Simulated and measured gain of the antenna at 122.5 GHz, E-Plane (left), H-plane (right)

1.2.4. Combination with a Bond Wire Compensation Structure and Integration into a Package

The feeding network of this antenna allows to directly integrate a bond wire compensation similar to [2]. The used compensation structure is optimized for three parallel bond wires in a distance of 100 µm. The length of the three wires is 350 µm. In that case an impedance of Z_X = (290 + j180) Ω results at the end of the bond contact pads. This impedance is compensated using two transmission lines.

A picture of the antenna with integrated bond wire compensation is shown in Figure 5. The antenna is glued into a 7 mm × 7 mm Quad Flat No Lead (QFN) package and connected to a chip dummy using three bond wires. This chip dummy only contains a 50 Ω through line and thus allows to measure the antenna including the bond wire interconnect. The chip dummy was manufactured using Alumina. As Alumina has a high permittivity (9.9) similar to Silicon, it also allows to observe the effect of the high permittivity chip in vicinity of the antenna.

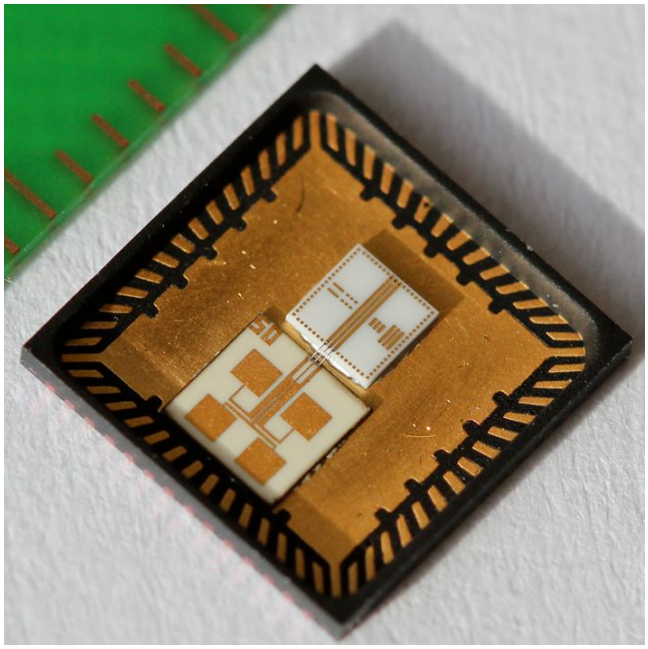

Figure 5 GCPW-fed antenna array with bond wire compensation

A comparison of the measured and simulated reflection coefficient of the antenna including the bond wire interconnect is shown in Figure 6. These show a very good agreement apart from a slight frequency shift. This can be attributed to the typical as-

sembly tolerances (die bonding, wire bonding). However, the measured reflection coefficient is below –10 dB in a frequency range of 117.5 GHz to 123.5 GHz and thus still covers the desired frequency range. This result confirms the reliability of the bond wire interconnect. The realative bandwidth is 5.0% and thus only slightly smaller compared to the antenna itself.

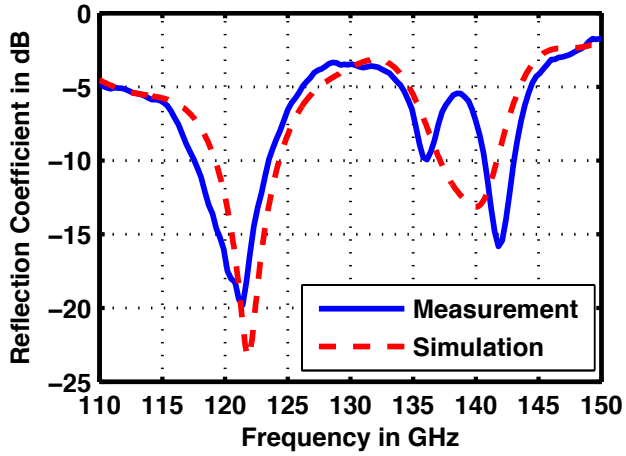

Figure 6 Simulated and measured reflection coefficient of the integrated antenna including the wire bond interconnect

The measured and simulated radiation patterns of the antenna including the bond wire interconnect are shown in Figure 7. Comparing the simulation results of the antenna only, and of the antenna with interconnect, the simulated antenna efficiency is reduced from 85% to 74%. The main lobe in the E-plane is slightly squinting towards the chip dummy (–3°). This is caused by the high permittivity of the chip dummy. The measured gain of the antenna with interconnect is 10.2dBi. The reduction can mainly be attributed to the transmission line loss on the chip dummy (0.5dB). Thus this confirms that the loss of the wire bond interconnect itself is below 0.5dB. Altogether, the integrated antenna still shows a very similar performance compared to the antenna only, although it is affected by the chip dummy, the wire bond interconnect and the plastic package. The sidelobes in the E-plane radiation pattern can again be attributed to reflections at the metallic waveguide probe.

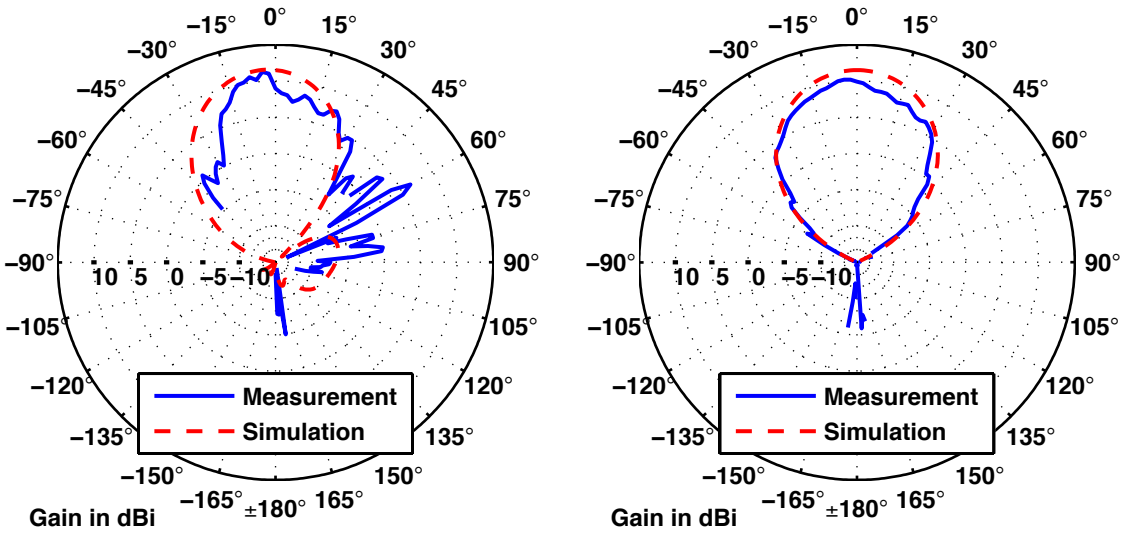

Figure 7 Simulated and measured gain of the integrated antenna inclusing the wire bond interconnect at 122.5 GHz, E-Plane (left), H-plane (right)

1.3. Bistatic 122 GHz Sensor in Bond Wire Technology

Figure 8 shows a 122GHz IC that is integrated into a 8 mm × 8 mm QFN package, together with two antennas. The IC and the antennas are connected using three aluminum wires in wedge-wedge technology. A detail view of the IC and the bond wires is shown in Fig. 8(b). The IC is 1.4 mm × 0.9 mm large and 0.25 mm high. It consists of the analog part of the IC that is presented in [8]. The voltage controlled oscillator (VCO) has a tuning range of 120.6 GHz to 124.3 GHz. This signal is fed through a power amplifier (PA) and then to the contact pads of the transmit antenna. The signal is also used to down-convert the received signal in an inphase-quadrature mixer. The IC also contains a 1/32 frequency divider that allows stabilizing the VCO with an external phase locked loop (PLL). Additionally, some temperature sensors and power detectors are implemented. In total, the IC has 22 contact pads that are connected to the leads of the QFN package using bond wires. The contact pads of the transmitter (upper edge of the IC) and of the receiver (right edge of the IC) are connected to the two antennas. The simulated radiation patterns of both antennas are similar to Fig. 6. The simulated antenna coupling is below –35 dB.

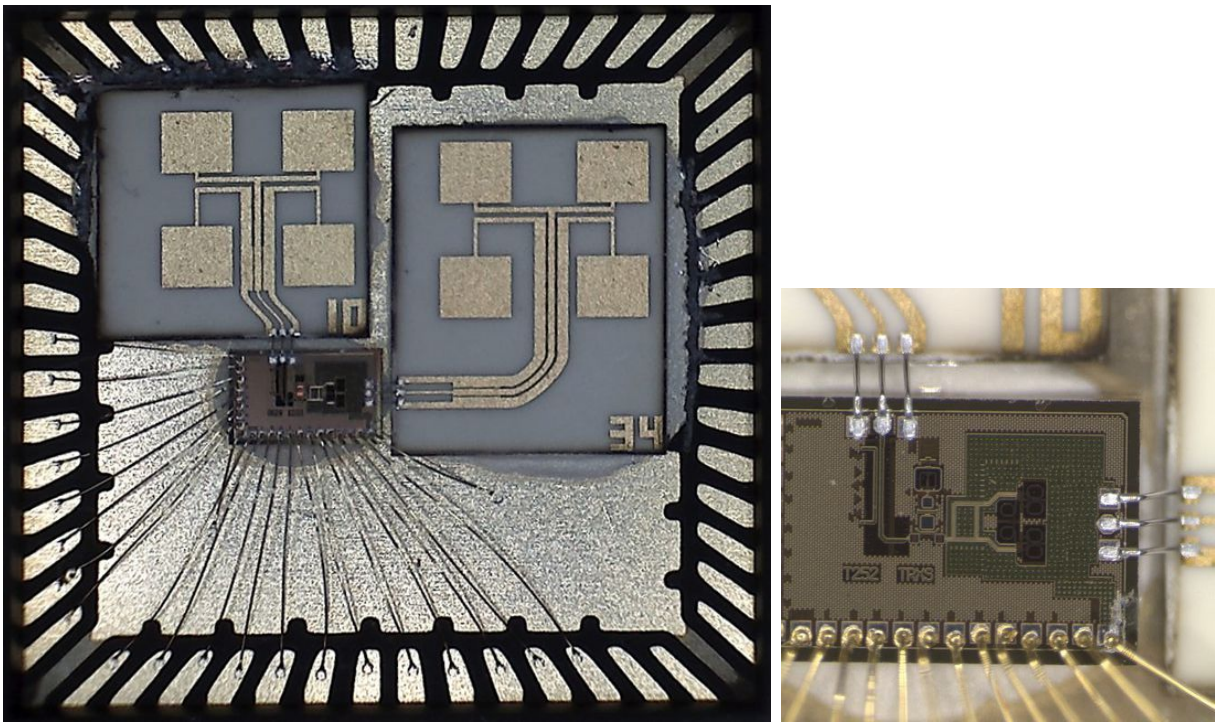

Figure 8 8 mm × 8 mm QFN package with integrated 122 GHz IC, transmit antenna (left), and receive antenna (right).

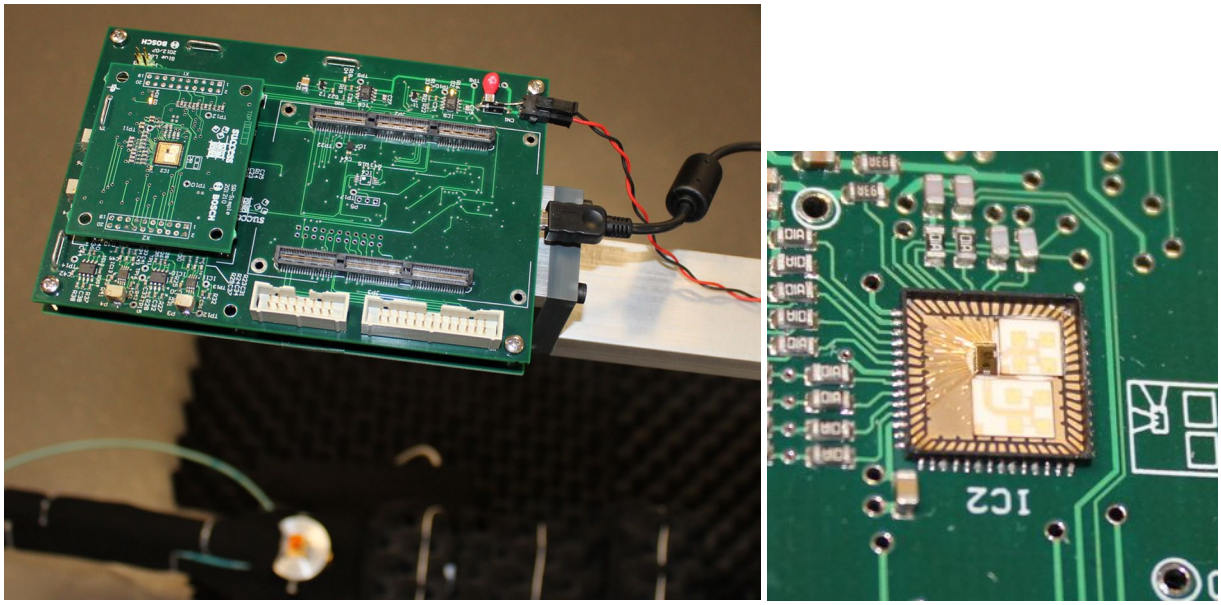

Figure 9 PCB in the measurement setup, and a detail view of the soldered sensor

Figure 9 PCB in the measurement setup, and a detail view of the soldered sensor shows a printed circuit board (PCB) that was developed to test the integrated Radar sensor. It allows controlling and analyzing the sensor. The PCB contains a PLL, power supply circuits and amplifiers for the down-converted receive signals. A close-up view

of the sensor that is soldered onto the PCB is also shown. As the IC and the bond wires need to be protected, a lid must be used to close the package. In this work, a ceramic lid (Alumina) with a thickness of 381 µm is used. As this is close to half a guided wavelength at 122 GHz, the reflected waves at the two interfaces air-dielectric and dielectric-air are effectively cancelled out [3].

The PCB was placed into the center of the probe based antenna measurement system at KIT to measure the radiation pattern of the transmit antenna. Therefore, the waveguide probe was demounted, and only the receive part of the measurement setup was used. The sensor was used as transmitter, stabilized by the PLL. During the measurements of both radiation patterns, the VCO frequency only varied from 121.103 GHz to 121.110 GHz. The receive horn antenna of the measurement setup was rotated around the sensor to record the radiation patterns. During this measurement the sensor was covered with the ceramic lid. The measurement results (compared to simulations) are shown in Figure 10. An excellent agreement can be observed. The slightly unsymmetric shape of the E-plane radiation pattern is caused by the ceramic lid and the fact that the antenna is positioned close to the package wall.

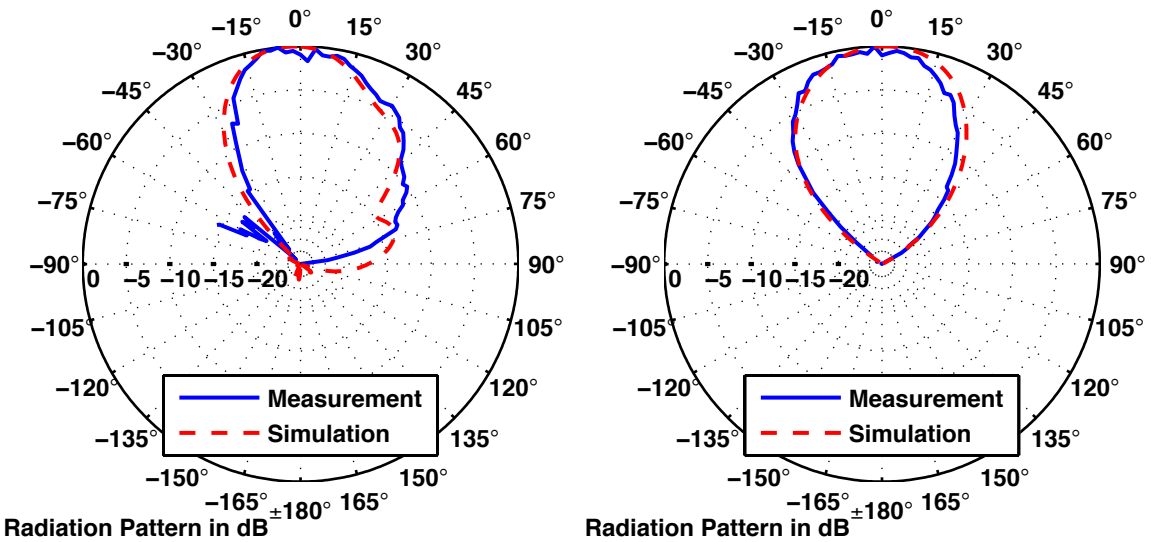

Figure 10 Simulated and measured radiation patterns of the sensor's transmit antenna. The sensor is covered with the ceramic lid.

2. AiP Solution using Flip Chip Bonding

2.1. Package Concept

The package concept is depicted in Figure 11. The package was fabricated using LTCC technology. It has a cavity in its center into which the MMIC is placed. A thermal conductive epoxy is used in between the MMIC and the package base to transfer the heat from the chip to the outside of the package. The thermal conductive adhesive can at the same time equalize a certain tolerance of the cavity depth. The antenna substrate is placed above the MMIC and connected to the MMIC using flip chip technology. Thus a high performance and broadband millimeter-wave interconnect is realized. The antenna itself is situated above an air cavity and uses the center die pad of the package as a reflector. Hence the desired radiation direction through the top of the package is achieved. The antenna substrate is also used for redistributing all signals leading to and from the MMIC to the package. Conductive epoxy bonding is used in between the antenna substrate and the package to conduct all signals and to fix the antenna substrate. Optionally, a cap can be placed on the package to protect the IC and the antenna. A detailed description of the package concept, the assembly process and the antenna functionality can be found in [9].

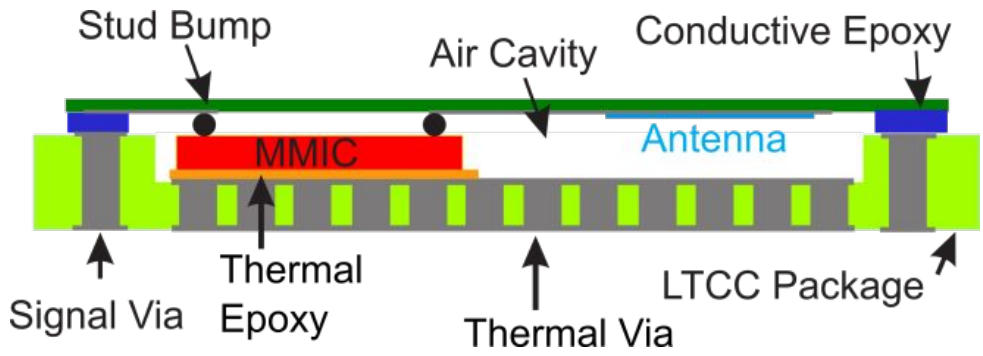

Figure 11 Cross section of the package layout

2.2. Double Dipole Antenna on a Flexible Polyimide Substrate

2.2.1. Antenna Design and Flip Chip Compensation

Strip antennas such as simple dipoles are favoured as a good performance can be achieved for the antenna/reflector configuration. A dipole is a symmetric antenna and therefore needs a symmetric feed. If fed by a coplanar waveguide a balun [10] is needed. A simple way to eliminate the need of a balun comes with the use of a double dipole array. In that case, the CPW line is separated into two coplanar striplines (CPS), that feed two dipoles directly [11]. This also improves the antenna performance as the radiation parallel to the substrate is minimized if the two dipoles are arranged in the correct distance to each other. A beamforming that enhances the radiation into the desired direction is therefore achieved in comparison to a single dipole antenna. Folded dipoles are used as the characteristic impedance of a printed dipole usually is below 40 Ω. CPS feed lines however can only be realized with a line impedance above 90 Ω. Folded dipoles lead to higher antenna impedances and additionally to several ways that allow tuning the antenna impedance [12]. Additional parasitic patch elements to reduce unwanted surface waves were used in the older designs with Alumina as the antenna substrate [1], [3]. This is not necessary now, as a low permittivity, and very thin antenna substrate is used. The antenna's geometric dimensions are given in Figure 12. The two dipoles are arranged in a distance of half a free-space wavelength to achieve the best radiation performance. The dipole length is 0.96 mm. When the antenna is assembled to the package, the reflecting die pad has a distance of 0.32 mm to the antenna.

The two folded dipoles have a characteristic impedance of Z_{fd} = 160 Ω. The CPS line impedance is also 160 Ω and thus the in- put impedance of the antenna at the CPW line is Z_{ant} = 80 Ω. This impedance has to be matched to the output impedance of the MMIC (50Ω). Additionally, any mismatch caused by the flip chip interconnect has to be compensated. The flip chip interconnect can be described as a transmission line, formed by the three metallic bumps [2]. Here, three bumps with a diameter of 60µm

are placed in a pitch of 100 µm. Besides the impedance transformation of this transmission line, other effects have to be considered for a flip chip interconnect. The metallic contact pads of the upper and lower chip lead to a capacitive load. Additionally, the permittivity of the upper substrate leads to a dielectric detuning of the transmission. The effect of the flip chip interconnect is compensated using a single transmission line. This transmission line directly matches to the antenna impedance of 80 Ω.

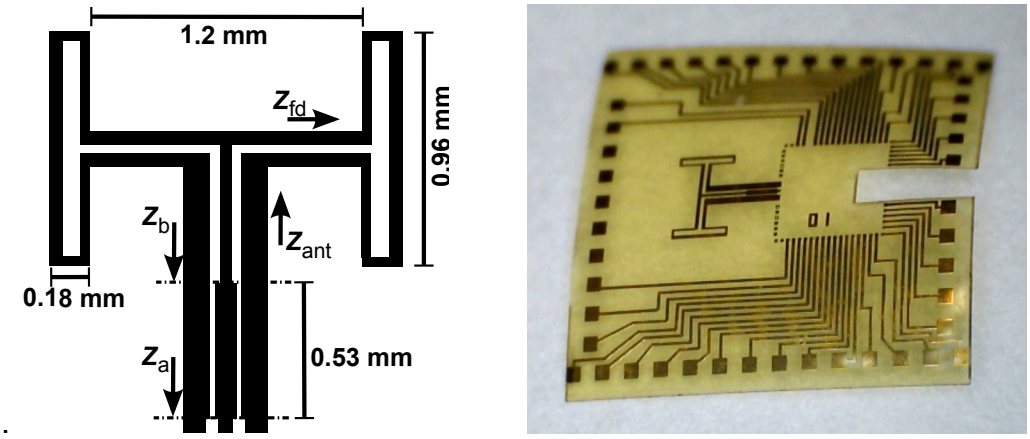

Figure 12 Polyimide substrate with antenna and chip-to-package redistribution

2.2.2. Influence of the redistribution lines

As the DC and signal redistribution lines are positioned on the same layer as the antenna itself, they might affect the antenna performance. Simulations show that as long as a safety margin is kept, the influence is negligible. The reflection coefficient remains below -20 dB within the targeted frequency range as long as the distance between the antenna and the lines is at least 0.4 mm. Concerning the radiation patterns, a slight gain degradation can be observed if the lines become too close. The gain is reduced by 0.5 dB and 1.0 dB when the distance is 0.5 mm and 0.2 mm, respectively. For the presented prototype, an area of 2.5 mm x 2.9 mm around the antenna is left free of metallic lines. Thus the distance between the antenna edges and the first line is 0.77 mm.

2.2.3. Antenna-in-Package Prototype

In a first step, a dummy chip that only contains a through-line was integrated into the package and connected to the antenna. Thus it is possible to measure the antenna

performance including the flip chip interconnect using a coplanar RF probe. A picture of this prototype is shown in Figure 13.

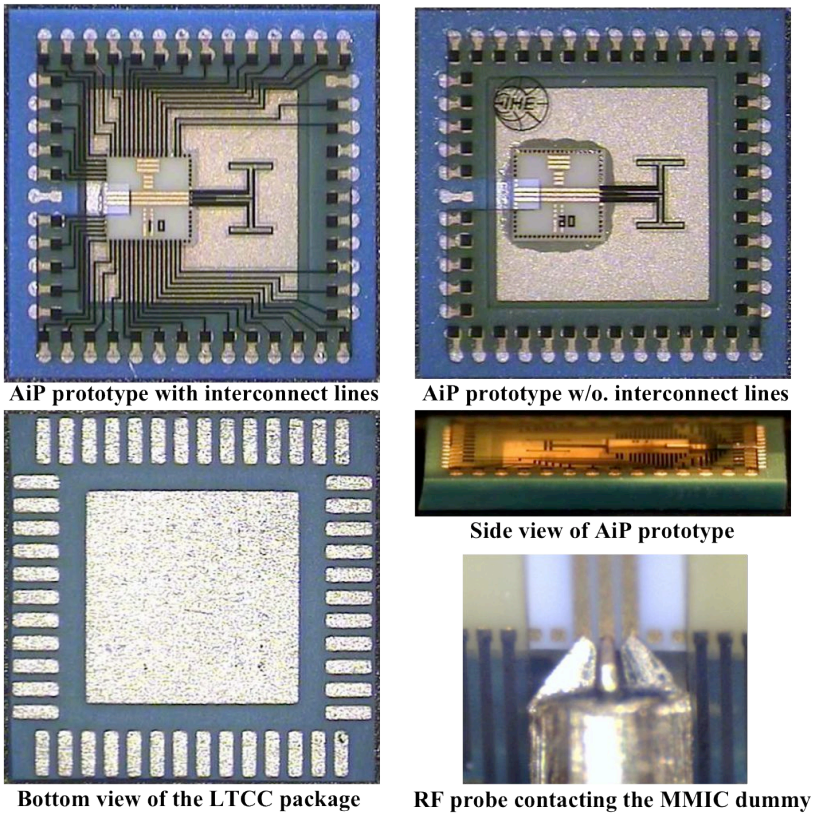

Figure 13 Antenna-in-Package Prototype

A very good agreement can be observed between the measured and simulated reflection coefficient of the antenna including the flip chip interconnects, as shown in Figure 14. A repeatability test was performed by fabricating seven different samples of the antenna, out of which two were fabricated without the interconnect lines on the antenna substrate. A high repeatability can be observed in the frequency range from 115 GHz to 126 GHz with slight variations above 126 GHz.

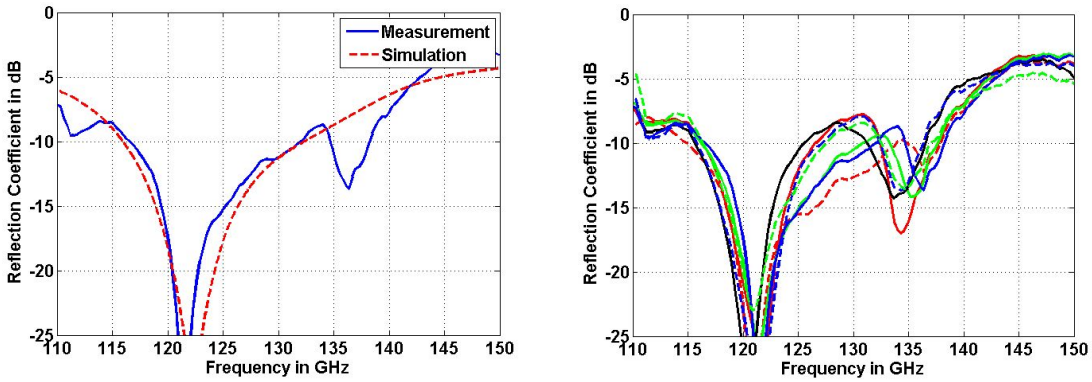

Figure 14 Simulated and measured reflection coefficient (left) and comparison of the measurements of seven different samples (right)

The measured and simulated radiation patterns are depicted in Figure 15. An excellent agreement has been achieved in both planes. The E-plane radiation pattern is affected by some reflections at the metallic waveguide probe and by a shadowing due to the probe in the angular range below -15°. The antenna shows the desired performance with a unidirectional radiation pattern and no sidelobes. The radiation patterns of both planes are similar. In summary, an antenna performance was achieved that is optimally suited for miniaturized radar sensors. It has a broad impedance bandwidth that can tolerate typical process inaccuracies and a radiation pattern without sidelobes.

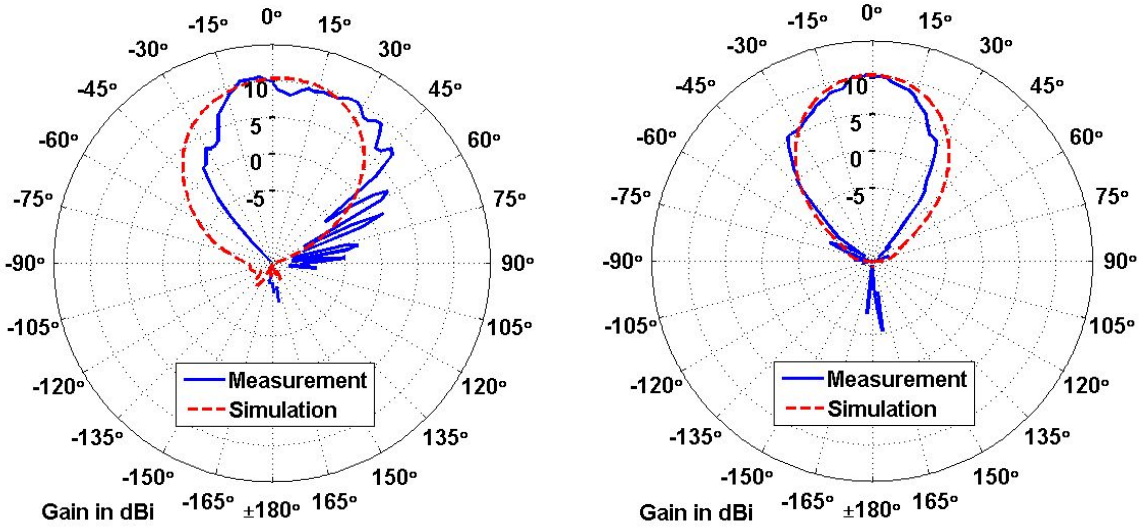

Figure 15 Radiation patterns of the AiP prototype at 122.5 GHz. E-plane (left), H-plane (right)

2.3. Bistatic Sensor in Flip Chip Technology

A fully integrated radar sensor is shown in Figure 16. It consists of a mixed signal 122-

GHz radar IC with separate connections for transmit and receive antennas[13]. The IC is 1.8 mm x 2.2 mm large and 0.25 mm thick. It has 70 contact pads in a pitch of 0.1 mm. These are connected to the package pads using metallic lines on the antenna substrate. The two antennas (double dipole antennas) are connected to the IC using flip chip technology. The double dipole antennas use the metallic pad in the center of the package as a reflector and thus radiate to the top. The whole package can be surface mounted on a standard PCB using a typical soldering process.

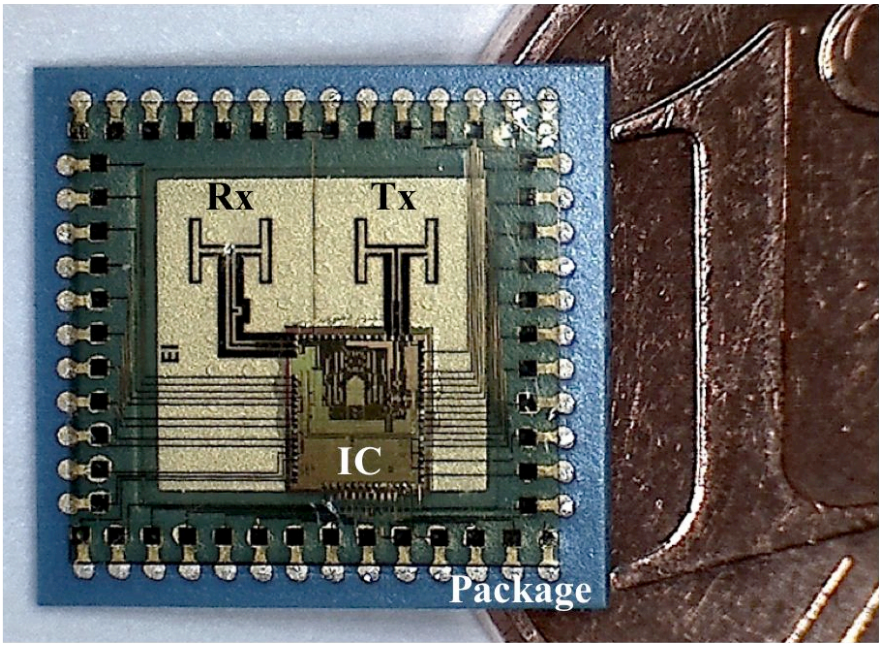

Figure 16 Fully integrated radar sensor in a (8 mm)^2 surface-mountable package beside a Euro-cent coin

The antenna design had to be slightly adapted to allow integrating two antennas into the chip package. The main difference is the reduced spacing of the two dipoles that form the double dipole antenna. This distance is now 0.98 mm instead of 1.38 mm. Additionally, a 90° bend was included into the feeding line of the receive antenna. The distance between the transmit and the receive antenna is 2.3 mm.

To verify the functionality and performance of the packaged radar sensor, a test board has been designed, which contains supply and biasing voltages, an SPI connector and miniaturized coaxial RF connectors to capture the signals coming out of the chip. The SPI communication between the mixed-signal radar transceiver and a PC is carried on using a custom Hi-Speed USB module. At the time of these measurements, the sensor could not be soldered onto the board, but was fixed to the board using a test socket.

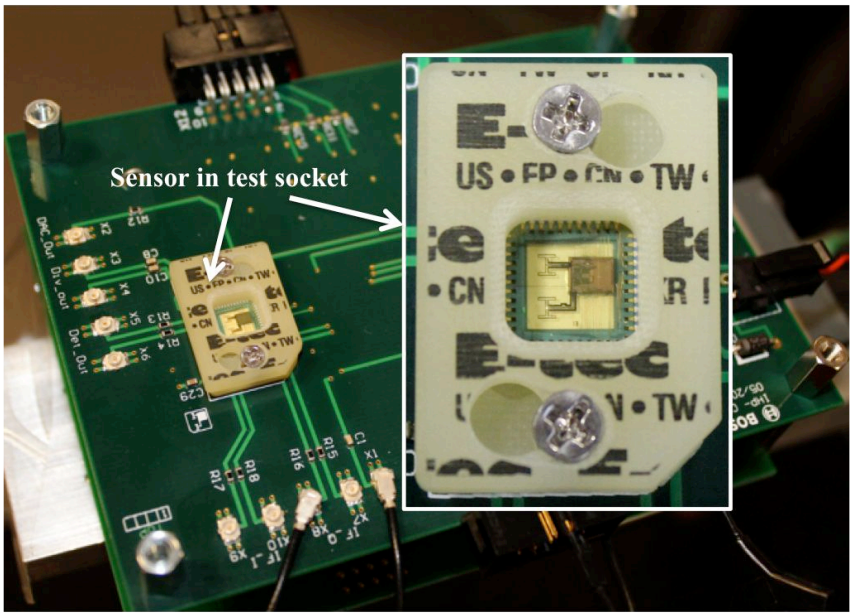

Figure 17 Test board and Radar sensor in a test socket

To measure the integrated antenna, the test board and the sensor was placed into the center of the antenna measurement setup. Instead of probing the antenna, the sensor is used as transmitter and the rotating horn antenna of the setup is receiving the radiated signal. In that case, the network analyzer is only receiving the signal while all its own sources are switched off. Thus a relative radiation pattern of the sensor's transmit antenna can be recorded. Although no PLL is used the sensor's VCO frequency only shifted between 119.320 GHz and 119.335 GHz during the measurement of the two planes and is thus nearly static.

The recorded radiation patterns are shown in Figure 18 in comparison to simulation results. The influence of the test socket can clearly be observed. It partly shadows the radiation in both planes in an angular range above +15°. This is caused by the position of the transmit antenna. Compared to Figure 15, the radiation patterns are broader. This can be attributed to the reduced antenna aperture that also leads to a lower antenna gain (8 dBi).

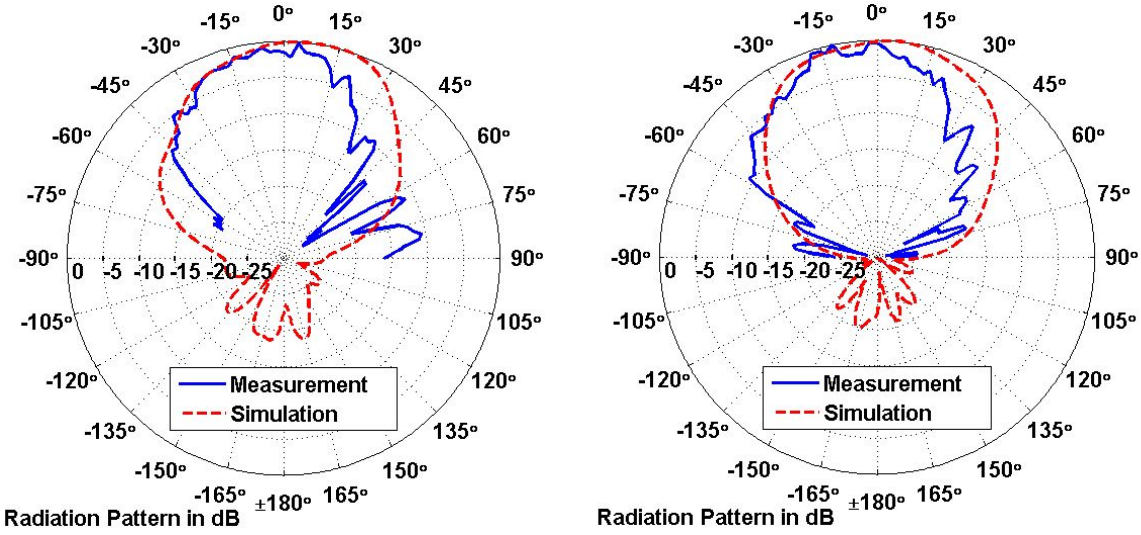

Figure 18 Radiation patterns of the sensors transmit antenna at 119.3 GHz. E-plane (left), H-plane (right)

3. Bibliography

[1] "Report on Package and Antenna Concepts," Deliverable 3.1, EU Project SUCCESS, Nov. 2010

[2] "Definition of Interconnect Solutions, Short Report," Deliverable 3.2, EU Project SUCCESS, Jan. 2011

[3] "Selection of Antenna Solutions, Short Report," Deliverable 3.3, EU Project SUCCESS, Mar. 2011

[4] D. Thompson, O. Tantot, H. Jallageas, G. Ponchak, M. Tentzeris, and J. Papapolymerou, "Characterization of liquid crystal polymer (LCP) material and transmission lines on LCP substrates from 30 to 110 GHz," IEEE Transactions on Microwave Theory and Techniques, vol. 52

[5] Y. Lu, Y. Huang, K. Teo, N. Sankara, W. Lee, and B. Pan, "Characterization of dielectric constants and dissipation factors of liquid crystal polymer in 60-80 GHz band," in IEEE Antennas and Propagation Society International Symposium, pp. 1 –4, July 2008.

[6] C. A. Balanis, Antenna theory: analysis and design. Hoboken, N.J.: Wiley-Interscience, 3. ed. ed., 2005.

[7] S. Beer and T. Zwick, "Probe based radiation pattern measurements for highly integrated millimeter-wave antennas," in European Conference on Antennas and Propagation, pp. 1 –5, April 2010.

[8] W. Debski, W. Winkler, Y. Sun, M. Marinkovic, J. Börngräber, and J. Scheytt, "120 GHz Radar mixed-signal transceiver," in European Micro-

wave Integrated Circuits Conference, Oct. 2012.

[9] S. Beer, H. Gulan, C. Rusch, T. Zwick," Integrated 122-GHz Antenna on a Flexible Polyimide Substrate with Flip Chip Interconnect", *IEEE Transactions on Antennas and Propagation*, in press

[10] S. Kim, S. Jeong, Y. Lee, D.-H. Kim, J.-S. Lim, K.-S. Seo, and S. Nam, "Ultra-wideband (from dc to 110 GHz) cpw to cps transition," Electronics Letters, vol. 38, pp. 622–623, June 2002.

[11] T. Zwick, D. Liu, and B. Gaucher, "Broadband planar superstrate antenna for integrated millimeterwave transceivers," IEEE Transactions on Antennas and Propagation, vol. 54, pp. 2790–2796, Oct. 2006.

[12] R. Lampe, "Design formulas for an asymmetric coplanar strip folded dipole," IEEE Transactions on Antennas and Propagation, vol. 33, pp. 1028–1031, Sep. 1985.

[13] Y. Sun, M. Marinkovic, G. Fischer, W. Winkler, W. Debski, S. Beer, T. Zwick, M. G. Girma, J. Hasch, C. J. Scheytt, " A Low-Cost Miniature 120 GHz SiP SiP FMCW/CW Radar Sensor with Software Linearization", *International Solid-State Circuits Conference,* Feb. 2013.